Published in final edited form as:
Bioorg Med Chem Lett. 2011 September 15; 21(18): 5470–5474. doi:10.1016/j.bmcl.2011.06.132.

SAR Analysis of Innovative Selective Small Molecule Antagonists of Sphingosine-1-Phosphate 4 ($S1P_4$) Receptor

Mariangela Urbano[a], **Miguel Guerrero**[a], **Jian Zhao**[a], **Subash Velaparthi**[a], **Marie-Therese Schaeffer**[b,d], **Steven Brown**[b,d], **Hugh Rosen**[b,c,d], and **Edward Roberts**[a,b,*]

[a]Department of Chemistry, The Scripps Research Institute, 10550 N. Torrey Pines Rd, La Jolla, CA 92037, United States

[b]Department of Chemical Physiology, The Scripps Research Institute, 10550 N. Torrey Pines Rd, La Jolla, CA 92037, United States

[c]Department of Immunology, The Scripps Research Institute, 10550 N. Torrey Pines Rd, La Jolla, CA 92037, United States

[d]The Scripps Research Institute Molecular Screening Center, 10550 N. Torrey Pines Rd, La Jolla, CA 92037, United States

Abstract

Recent evidence suggests an innovative application of chemical modulators targeting the $S1P_4$ receptor as novel mechanism-based drugs for the treatment of influenza virus infection. Modulation of the $S1P_4$ receptor may also represent an alternative therapeutic approach for clinical conditions where reactive thrombocytosis is an undesired effect or increased megakaryopoiesis is required. With the exception of our recent research program disclosure, we are not aware of any selective $S1P_4$ antagonists reported in the literature to date. Herein, we describe complementary structure-activity relationships (SAR) of the high-throughput screening (HTS)-derived hit 5-(2,5-dichlorophenyl)-*N*-(2,6-dimethylphenyl)furan-2-carboxamide and its 2,5-dimethylphenyl analog. Systematic structural modifications of the furan ring showed that both steric and electronic factors in this region have a significant impact on the potency. The furan moiety was successfully replaced with a thiophene or phenyl ring maintaining potency in the low nanomolar range and high selectivity against the other S1P receptor subtypes. By expanding the molecular diversity within the hit-derived class, our SAR study provides innovative small molecule potent and selective $S1P_4$ antagonists suitable for *in vivo* pharmacological validation of the target receptor.

Keywords

$S1P_4$ receptor antagonists; $S1P_{1\text{-}3,5}$ receptor family; megakaryocyte differentiation; viral infections

Sphingosine-1-phosphate (S1P) is a pleiotropic lysophospholipid involved in a wide range of cellular functions including proliferation, apoptosis, differentiation and migration.[1–6]

*Corresponding author. eroberts@scripps.edu, Phone: +1 858 784 2396, FAX: +1 858 784 2988.

High levels of S1P are present in lymph (30 nM to 300 nM) and plasma (100 nM to 1 μM), whereas those found in tissues are significantly lower.[7] Although platelets possess the highest sphingosine kinase activity, accumulating evidence suggests that the plasma levels of S1P are mainly the result of its release from erythrocytes due to their great number, capability to store S1P produced from other tissues, and lack of S1P-degrading enzymes. Furthermore, mast cells have been described as additional vascular source of S1P upon IgE dependent activation, while the vascular endothelium could be the main source of lymph S1P.[7,8]

S1P can function intracellularly as a second messenger or extracellularly by binding with nanomolar affinities to five S1P G-protein coupled receptor subtypes named $S1P_{1,2,3,4,5}$ (formerly $Edg_{1,5,3,6,8}$ receptors).[9–10] $S1P_{1–5}$ members share approximately 40% sequence identity, with a conserved glutamic acid residue at the third transmenbrane domain responsible for the ligand specificity *versus* the closely related lysophosphatidic acid (LPA) $Edg_{2,4,7}$ receptors family.[11] The coupling of $S1P_{1–5}$ to different signaling cascades along with their differential expression pattern explains the broad biological effects of S1P. $S1P_1$ is expressed ubiquitously, particularly in brain, lung, spleen, heart, liver as well in a variety of immune system cells lineages.[7] High affinity $S1P_1$ agonists have been widely studied and emerged as major immunomodulatory molecules with therapeutic applications being tested in multiple sclerosis and allogenic transplantation.[12] $S1P_3$ is also widely distributed with highest levels in the heart where it is co-expressed with $S1P_1$ and $S1P_2$. $S1P_2$ has been shown to be expressed in rat brain during embryogenesis as well as in most other developing tissues. $S1P_5$ is highly present in adult rat brain, while in human and mouse high expression of the receptor is also found in the spleen. [13]

$S1P_4$ has been shown to bind S1P with lower affinity and have a narrower tissue distribution than the other family members. First isolated from human and mouse dendritic cells (DCs), $S1P_4$ is highly expressed in lymphoid and hematopoietic tissue.[13] $S1P_4$ have been reported to couple to $G\alpha_{i,}$ $G\alpha_o$ and $G_{\alpha 12/13}$ proteins leading to the stimulation of MAPK/ERK signaling pathways, as well as PLC and Rho-Cdc42 activation.[14–15] Molecules targeting S1P-metabolizing enzymes have been recently proposed as innovative potential therapeutics for viral diseases.[1,12a,16] Consistent with these data, local S1P receptor modulation in the lung has been demonstrated to control immunopathological features of influenza virus infections by impairing the accumulation of DCs and cytokine release in the draining lymph nodes without altering the essential activity of virus-specific T-cells toward virus-infected cells.[12a] Therefore, regulation of pulmonary immune response by S1P receptor modulators may have therapeutic implications for alleviating excessive immune response responsible for exacerbating airway diseases. Based on the evidence that modulation of $S1P_1$ alone did not inhibit DC-dependent T cell activation, and that the sphingosine analog used in the experiments did not bind to $S1P_2$, it was hypothesized that either the single activation of $S1P_3$, $S1P_4$, $S1P_5$ or the combined activity on $S1P_{1,3,4,5}$ is responsible for the functional impairment of DCs.[12a] Reports showing that, in contrast to $S1P_5$ and $S1P_2$, $S1P_4$ is highly expressed in DCs[10] confirm that the $S1P_4$ chemical activation in the airway may be effective at controlling the immunopathological response to viral infections, thus offering novel mechanism-based potential therapeutics for airway viral diseases.

Both *in vitro* and *in vivo* experiments have recently provided strong evidence that $S1P_4$ is involved in the late stage of megakaryocyte differentiation. In $S1P_4$–deficient mice the bone marrow is characterized by the presence of morphologically aberrant megakaryocytes, and platelet repopulation of the peripheral blood after thrombocytopenia is delayed. Indeed, $S1P_4$ has been proposed as a suitable target either for increasing thrombocyte production in clinical conditions requiring increased platelets number, or for inhibiting a potentially detrimental reactive thrombocytosis.[8]

Despite the emerging therapeutic potential, aspects of the biological role of $S1P_4$ remain unclear, partly due to the lack of ligands with high selectivity against the $S1P_{1–3,5}$ subtypes. Herein we report on the synthesis, biological evaluation and structure-activity relationships (SAR) of the first class of selective $S1P_4$ antagonists.

Recently, investigations from our laboratories have led to the discovery of the first class of potent and selective $S1P_4$ antagonists.[17] Synthesis and SAR analysis of various derivatives based on a 5-aryl furan-2-arylcarboxamide scaffold were carried out on regions A and C of the original hit **1a** identified through a high-throughput screening campaign (Figure 1, Table 1). Similar biological properties were found for the 2,5-dimethylphenyl analog **1b** (Figure 1). It was postulated that disubstitution on positions 2 and 6 of the phenyl ring C with small alkyl groups (e.g. methyl, ethyl) was essential to increase the potency. Remarkably, steric and electronic effects at position 4 of the phenyl ring C did not affect the functional activity to any appreciable extent, thus allowing the installation of solubility enhancing features such as alcohols and amines. However, safety concerns might arise from the presence of the furan ring given the number of furan-containing drug candidates demonstrating hepatotoxic and hepatocarcinogenic effects as a result of furan cytochrome P450-catalyzed oxidative metabolism and the covalent binding of the electrophilic metabolites to macromolecules.[18] Thus, our chemistry efforts were successively focused on the SAR analysis of the central moiety B with the aim to acquire more insight into the receptor binding mode and identify new chemotypes to address potential metabolic and toxicity issues. For investigational purposes we fragmented the moiety B into aryl ring **d** and amide group **e** (Figure 1) while conserving regions A and C as in **1a** and **1b**.

In our previous studies[17] it was hypothesized that the hydrogen-bond donor capability of the amide group was important for the functional activity. Herein, the impact of the carbonyl group as hydrogen-bond acceptor was explored by replacing the amide functionality by a methyleneaniline as in **5**. Suzuki coupling[19] between bromide **2** and boronic acid **3** followed by reductive amination with 2,6-dimethylaniline **4** furnished the final compound **5** (Scheme 1).

Notably, **5** was found to be inactive in the $S1P_4$ antagonist assay,[20] indicating that the amide function is an essential molecular feature in the binding mode.

A systematic SAR analysis of the furan ring **d** was performed by the synthesis of molecules containing variously substituted aromatic rings as outlined in Schemes 2–9. Initially, the furan ring was replaced by 1,3,4-oxadiazole as a substructure with potentially improved toxicity profile[18] (**9**, Scheme 2). Condensation of hydrazide **6** with ethyl oxalyl chloride **7** followed by cyclization using Burgess reagent afforded oxadiazole ethyl ester **8**. Subsequent ester hydrolysis of **8** followed by amidation with **4** furnished the final compound **9**.

Aware of literature evidence of pyrrole and thiophene toxicity which mostly arises from hydroxylation at C2 and C5 positions,[18] *N*-methyl pyrrole **14** and thiophene **19** analogs were prepared (Schemes 3, 4) primarily to elucidate the electronic effects of the oxygen atom on the functional activity. Suzuki coupling of phenyl iodide **10** with *N*-Boc-pyrrole boronic acid **11** furnished the *N*-deprotected pyrrole **12** as the major product.[19] Alkylation of **12** with methyl iodide under strong basic conditions followed by hydrolysis of the methyl ester afforded carboxylic acid **13**. Coupling the acyl chloride of **13** with **4** furnished compound **14**.

The synthesis of intermediate **17** commenced with the esterification of carboxylic acid **15** followed by Suzuki coupling with 2,5-dimethylphenyl boronic acid **16**. Ester hydrolysis of **17**, formation of the acyl chloride and coupling with **4** furnished thiophene derivative **19** (**CYM50333**) (Scheme 4).

As regioisomers of **1b**, 5-aryl furan-3-carboxamide **23** and 4-aryl furan-2-carboxamide **28** were synthesized in order to elucidate the electronic requirements of the 5-membered ring **d**, while keeping the pendant regions A and C geometrically similar to **1a** and **1b**. The synthesis of **23** is depicted in Scheme 5. Esterification of **20** followed by Suzuki coupling with boronic acid **16** afforded **22**. Subsequent ester hydrolysis, formation of acyl chloride and coupling with **4** provided the desired compound **23**.

The 4-arylfuran-2-carboxamide **28** was synthesized as shown in Scheme 6. Selective debromination of **24** followed by esterification and Suzuki coupling afforded the 4-arylfuran-2-methyl ester **27**. Synthesis of **28** was finally achieved by ester hydrolysis of **27**, formation of acyl chloride and subsequent coupling with aniline **4**.

Successively, a methyl group was inserted either on position 3 or 4 of the furan ring in order to evaluate the steric requirements of region B as well as conformational restrictions on the pendant regions A and C. Trisubstituted furans **33** and **37** were synthesized as illustrated in Scheme 7 and 8. Bromination of furan **29**, followed by Suzuki coupling with boronic acid **16** afforded ester **31**. Ester hydrolysis followed by acyl chloride preparation and amide coupling with **4** yielded the desired furan **33** (Scheme 7).

Synthesis of the regioisomer **37** involved a selective Suzuki coupling between dibromo furan **34** and boronic acid **16** followed by methylation through Stille coupling,[21] hydrolysis of ester **36**, and coupling of the acyl chloride derivative with aniline **4** (Scheme 8).

Finally, new chemical space was explored by replacing the furan ring with phenyl and pyridine as potential 6-membered ring bioisosteres. The synthesis is depicted in Scheme 9. Suzuki coupling of phenylboronic acids (**3** or **16)** with the appropriate bromo phenyl (**38** or **39)** or pyridine **40** derivatives afforded the corresponding biaryl esters **41–43**. Successively, ester hydrolysis, acyl chloride formation and amide coupling with aniline **4** furnished the desired products **47** (**CYM50367**), **48**, **49**.

The $S1P_4$ functional antagonist activity of the aforementioned compounds is listed in Table 1. Surprisingly, the 2,5-disubstituted oxadiazole **9** was inactive. Similarly, the *N*-methyl-pyrrole **14** was 98-fold less potent than **1b**. Conversely, the thiophene was found to be a suitable bioisoster of the furan ring, with the 2,5-disubstituted thiophene analog **19** displaying similar potency to the hit and **1b**. Furthermore, both regioisomers **23** and **28** were 3-fold less potent than **1b**. Trisubstituted furan regioisomers **33** and **37** were respectively 3- and 14-fold less potent than **1b**; the loss of potency was attributed to unfavorable steric interactions of the methyl group with the receptor or resulting conformational modification of the molecule. Particularly, it was hypothesized that the methyl in **37** forces the biaryl C-C bond angle into a less active anti-coplanar conformation. Geometrically similar molecules **9**, **14**, **19**, **23** and **28**, having the amide group **e** and the ring A arranged in a 1,3 substitution pattern on the heteroaromatic central system **d**, displayed very different potencies suggesting that electronic effects are essential for the $S1P_4$ antagonist activity. Interestingly, the 1,3-disubstituted phenyl derivative **47** showed similar potency to **19**, **1a** and **1b**, whereas the pyridine analog **49** was inactive. The lack of activity of oxadiazole **9** and pyridine **49** suggested that heterocycles with basic lone pares at the ring **d** are detrimental to the potency. In agreement with the SAR trend within the furan derivatives, the methylated phenyl analog **48** was 32-fold less potent than the corresponding homolog **47**, supporting the hypothesis that a methyl group in the ring **d** *ortho* to the biaryl C-C bond is detrimental to the activity.

The most active compounds **19** and **47** were selected for functional assays at $S1P_{1–3,5}$ subtypes (Table 2). Notably, both compounds displayed an exquisite selectivity for the $S1P_4$ receptor *versus* the other receptor family subtypes.

In summary, a systematic SAR analysis was carried out on region B of the original hit **1a** and its analog **1b**. Structural modifications of the central ring **d** showed that electronic effects are fundamental for the activity, and revealed that a methyl substitution *ortho* to the C-C biaryl bond has a negative impact on the activity, perhaps by forcing the biaryl system into an anti-coplanar conformation. Interestingly, both thiophene and phenyl rings were found to be bioisosteres of the furan moiety, thus expanding the molecular diversity within the hit-derived molecules and including new chemotypes which may address potential metabolic/toxicity issues. Remarkably, compounds **19** (**CYM50333**) and **47** (**CYM50367**), as novel highly selective $S1P_4$ antagonists with low nanomolar activity, represent valuable small molecule tools to investigate the biological and pharmacological role of the target receptor in megakaryocyte differentiation and fundamental immune processes. Based on the acquired SAR of the explored regions (A, B, C),[17] additional studies are currently ongoing in our research group to improve the physicochemical properties and further increase the $S1P_4$ antagonist potency, while preserving the $S1P_{1–3,5}$ selectivity profile. Our research progresses will be communicated in due course.

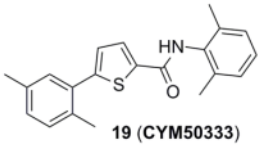

19 (**CYM50333**)

S1P receptor activity (IC_{50})

$S1P_4$ = 59 nM
$S1P_1$ > 25 μM
$S1P_2$ = 1.1 μM (40% inhibition)
$S1P_3$ = 35% (25 μM)
$S1P_5$ = 30% (25 μM)

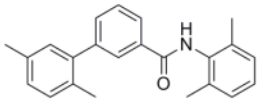

47 (**CYM50367**)

$S1P_4$ = 75 nM
$S1P_1$ = 30% (25 μM)
$S1P_2$ = 25% (25 μM)
$S1P_3$ = 40% (25 μM)
$S1P_5$ = 40% (25 μM)

Acknowledgments

This work was supported by the National Institute of Health Molecular Library Probe Production Center grant U54 MH084512 (ER, HR), and by AI074564 (Michael Oldstone, PI). We thank Mark Southern for data management with Pub Chem.

References and notes

1. Marsolais D, Hahm B, Walsh KB, Edelmann KH, McGavern D, Hatta Y, Kawaoka Y, Rosen H, Oldstone MB. Proc Natl Acad Sci USA. 2009; 106(5):1560. [PubMed: 19164548]
2. Marsolais D, Rosen H. Nat Rev Drug Discov. 2009; 8:297. [PubMed: 19300460]
3. Alfonso C, McHeyzer-Williams MG, Rosen H. Eur J Immunol. 2006; 36:149. [PubMed: 16342326]
4. Jo E, Sanna MG, Gonzalez-Cabrera PJ, Thangada S, Tigyi G, Osborne DA, Hla T, Parrill AL, Rosen H. Chem Biol. 2005; 12:703. [PubMed: 15975516]
5. Sanna G, Liao J, Jo E, Alfonso C, Ahn M, Peterson MS, Webb B, Lefebvre S, Chun J, Gray N, Rosen H. J Biol Chem. 2004; 279:13839. [PubMed: 14732717]
6. Wei SH, Rosen H, Matheu MP, Sanna MG, Wang S, Jo E, Wong C, Parker I, Cahalan M. Nat Immunol. 2005; 6:1228. [PubMed: 16273098]
7. López Almagro, R.; Tarrasón, G.; Godessart, N. Structure, Signaling, And Physiology. Cambridge University Press; Cambridge: 2011. Protein-Coupled Receptors.
8. Golfier S, Kondo S, Schulze T, Takeuchi T, Vassileva G, Achtman AH, Gräler MH, Abbondanzo SJ, Wiekowski M, Kremmer E, Endo Y, Lira SA, Bacon KB, Lipp M. FASEB J. 2010; 24:4701. [PubMed: 20686109]
9. Chun J, Goetzl EJ, Hla T, Igarashi Y, Lynch KR, Moolenaar W, Pyne S, Tigyi G. Pharmacol Rev. 2002; 54:265. [PubMed: 12037142]

10. Maeda Y, Matsuyuki H, Shimano K, Kataoka H, Sugahara K, Kenji Chiba K. J Immunol. 2007; 178:3437. [PubMed: 17339438]
11. Holdsworth G, Osborne DA, Pham TCT, Fells JI, Hutchinson G, Milligan G, Parrill AL. BMC Biochemistry. 2004; 5:12. [PubMed: 15298705]
12. (a) Marsolais D, Hahm B, Edelmann KH, Walsh KB, Guerrero M, Hatta Y, Kawaoka Y, Roberts E, Oldstone MB, Rosen H. Mol Pharmacol. 2008; 74:896. [PubMed: 18577684] (b) Brinkmann V, Billich A, Baumruker T, Heining P, Schmouder GF, Aradhye PB. Nat Rev Drug Discov. 2010; 9:883. [PubMed: 21031003]
13. Candelore MR, Wright MJ, Tota LM, Milligan J, Shei GJ, Bergstrom JD, Mandala SM. Biochem Biophys Res Commun. 2002; 297:600. [PubMed: 12270137]
14. Toman RE, Spiegel S. Neurochem Res. 2002; 27:619. [PubMed: 12374197]
15. Kohno T, Matsuyuki H, Inagaki Y, Igarashi Y. Genes Cells. 2003; 8:685. [PubMed: 12875654]
16. Seo YJ, Blake C, Alexander S, Hahm B. J Virol. 2010; 84:8124. [PubMed: 20519401]
17. Guerrero M, Urbano M, Velaparthi S, Zhao J, Schaeffer M-T, Brown S, Rosen H, Roberts E. Bioorg Med Chem Lett. 201110.1016/j.bmcl.2011.04.097
18. Dalvie DK, Kalguktar AS, Khojasteh-Bakht SC, Obach RS, O'Donnell JP. Chem Res Toxicol. 2002; 15:269. [PubMed: 11896674]
19. McAllister LA, Hixon MS, Kennedy KP, Dickerson TJ, Janda KD. J Am Chem Soc. 2006; 128:4176. [PubMed: 16568962]
20. The activity was measured by using Tango™ EDG6-bla U2OS cells which contain the human Endothelial Differentiation Gene 6 linked to a GAL4-VP16 transcription factor via a TEV protease site. The cells also express a beta-arrestin/TEV protease fusion protein and a beta-lactamase (BLA) reporter gene under the control of a UAS response element. BLA expression is monitored by measuring fluorescence resonance energy transfer (FRET) of a cleavable, fluorogenic, cell-permeable BLA substrate.
21. Bach T, Krüger L. Eur J Org Chem. 1999; 1999:2045.

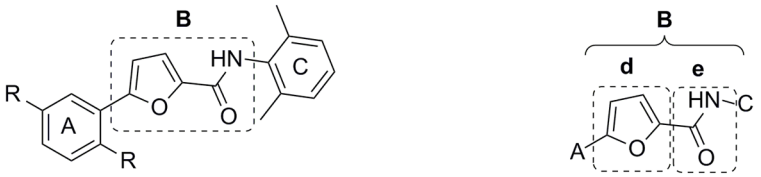

1a R = Cl	**1b** R = Me
Antagonist activity (IC_{50})	Antagonist activity (IC_{50})
$S1P_1$ > 20 μM	$S1P_1$ > 20 μM
$S1P_3$ > 20 μM	$S1P_3$ > 20 μM
$S1P_4$ = 78 nM	$S1P_4$ = 64 nM
$S1P_5$ = 14 μM	$S1P_5$ > 20 μM

Figure 1.
Novel $S1P_4$ antagonists based on a 5-aryl furan-2-arylcarboxamide scaffold

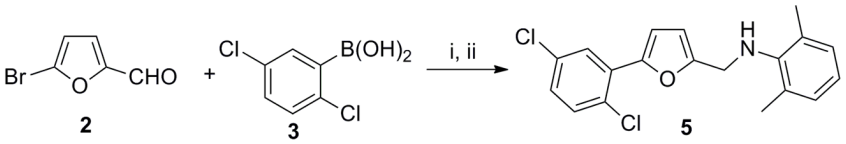

Scheme 1. Synthesis of aniline derivative 5

Reagents and conditions: (i) $Pd(PPh_3)_4$ (0.1 equiv), **3** (1.5 equiv), 2M aq. Na_2C0_3 (2 equiv), 1,4-dioxane, 80 °C. 12 h, 65%; (ii) **4** (1.2 equiv), $NaBH(OAc)_3$ (1.3 equiv), AcOH (1.5 equiv), DCE, rt, overnight, 75%.

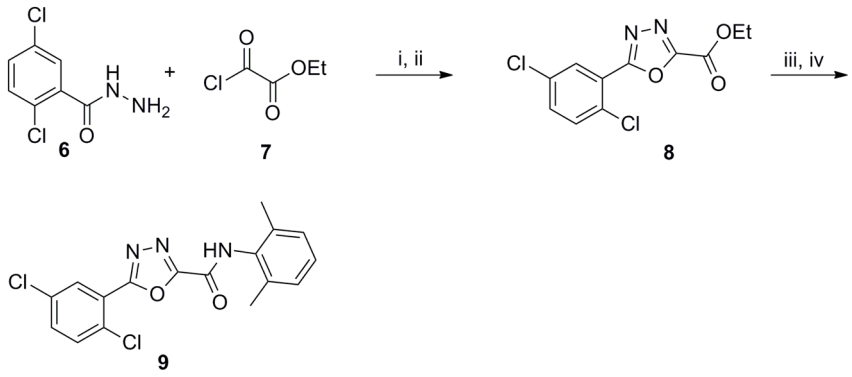

Scheme 2. Synthesis of 1,3,4-oxadiazole derivative 9

Reagents and conditions: (i) **7** (1.0 equiv), Et_3N (2 equiv), CH_2Cl_2, 0 °C, 1 h; (ii) Burgess reagent (1.5 equiv), THF, 80 °C, 10 h, 40% (over 2 steps); (iii) 2N aq. NaOH, MeOH, rt, 2 h; (iv) **4** (1.2 equiv), EDCl (1.2 equiv), HOBt (1.2 equiv), DMF, rt, overnight, 70 % (over 2 steps).

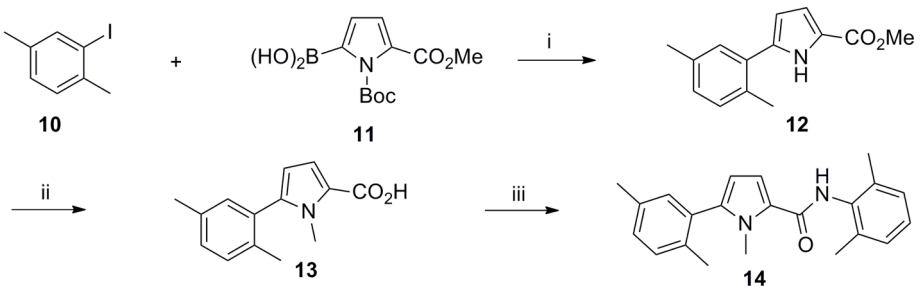

Scheme 3. Synthesis of *N*-methyl pyrrole analog 14

Reagents and conditions: (i) $Pd(PPh_3)_4$ (0.05 equiv), Na_2CO_3 (2 equiv), 1,4-dioxane/H_2O (10:1), 100 °C. 4 h, 50%: (ii) (a) Mel (1.5 equiv), NaH (1.5 equiv), DMF, 0 °C to rt, overnight, 65%: (b) LiOH (1.3 equiv), THF/MeOH/H_2O (2: 2: 1), rt, 2 h;(iii) (a) $(COCl)_2$ (1.3 equiv), DMF, CH_2Cl_2, 0 °C to rt, 8 h; (b) Et_3N (2 equiv), **4** (2 equiv), CH_2Cl_2, 0 °C, 2 h, 50% (over 3 steps).

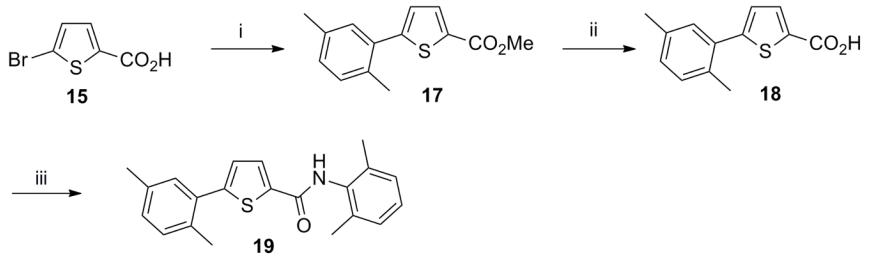

Scheme 4. Synthesis of thiophene analog 19

Reagents and conditions: (i) (a) conc. H_2SO_4, MeOH, reflux, 12 h; (b) $Pd(OAc)_2$ (0.05 equiv), Cy_3P (0.1 equiv), **16** (1.4 equiv), K_3PO_4 (3 equiv), toluene/H_2O (8:1), 100 °C, 12 h, 50% (over 2 steps): (ii) 1M aq. LiOH (1 equiv), THF, 24 h, 25 °C; (iii) (a) $(COCl)_2$ (1.3 equiv), DMF, CH_2Cl_2, rt, 8 h; (b) Et_3N (2 equiv), **4** (1.2 equiv), CH_2Cl_2, rt, overnight, 75% (over 3 steps).

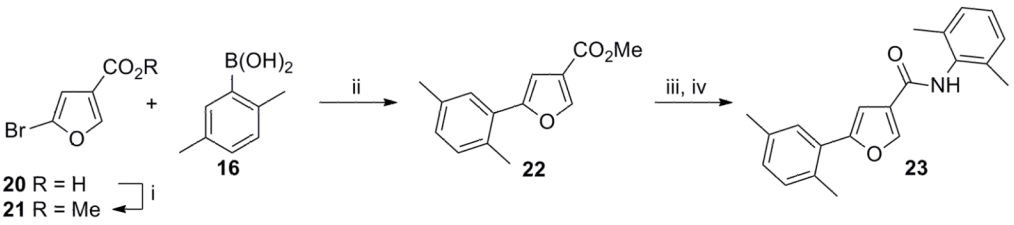

Scheme 5. Synthesis of 5-aryl furan-3-carboxamide regioisomer 23

Reagents and conditions: (i) conc. H_2SO_4, MeOH, reflux, 12h, 60%; (ii) **16** (1.5 equiv), $Pd(OAc)_2$ (0.05 equiv). Cy_3P (0.1 equiv), K_3PO_4 (3 equiv), toluene/H_2O (8:1), 100 °C, 12 h, overnight, 78%; (iii) LiOH (1.2 equiv), THF/MeOH/H_2O (2: 2:1), rt. 3 h; (iv) (a) $(COCl)_2$. DMF, CH_2Cl_2, rt, 8 h; (b) **4** (1.2 equiv), Et_3N(1.5 equiv), rt, overnight, 88% (over 3 steps).

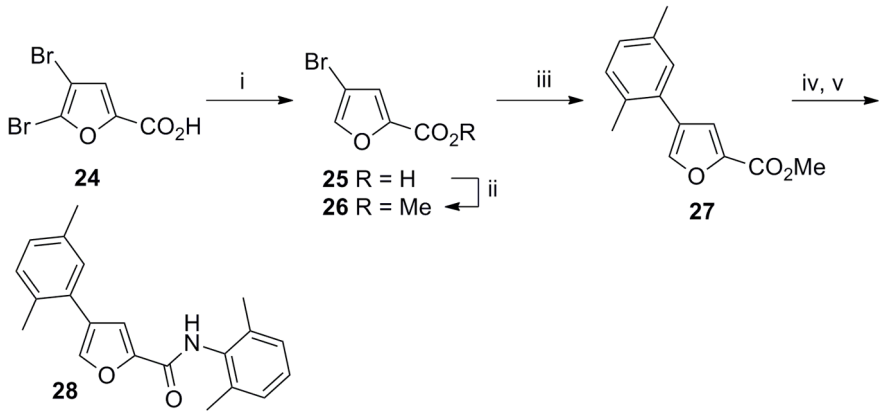

Scheme 6. Synthesis of 4-aryl furan-2-carboxamide regioisomer 28

Reagents and conditions: (i) aq. NH_4OH, Zn (1 equiv), rt, 3 h, 80%; (ii) conc. H_2SO_4, MeOH, reflux, 12 h, 90%; (iii) **16** (1.4 equiv), $Pd(OAc)_2$ (0.05 equiv), Cy_3P (0.1 equiv), K_3PO_4 (3 equiv), toluene/H_2O (8:1), 100 °C, 12 h, 60%; (iv) LiOH (1.3 equiv), THF/MeOH/H_2O (2: 2:1), rt, 3 h;(v) (a) $(COCl)_2$ (1.3 equiv), DMF, CH_2Cl_2, rt, overnight; (b) Et_3N (2.0 equiv), **4** (1.4 equiv), CH_2Cl_2, rt, 2 h, 85% (over 3 steps).

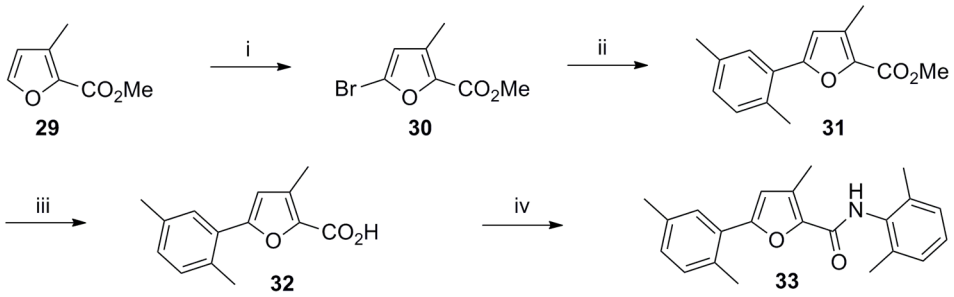

Scheme 7. Synthesis of 2,3,5-trisubstituted furan analog 33

Reagents and conditions: (i) NBS (1.1 equiv), MeOH/THF, 0 °C to rt, 2 h, 60%; (ii) $Pd(OAc)_2$ (0.05 equiv), Cy_3P (0.01 equiv), **16** (1.4 equiv), K_3PO_4 (3 equiv), toluene/H_2O (8:1), 100 °C, 12 h, 50%; (iii) LiOH (1.3 equiv), THF/MeOH/H_2O (2: 2:1), rt, 3 h; (iv) (a) $(COCl)_2$ (1.3 equiv), DMF, CH_2Cl_2, rt, overnight: (b) Et_3N (2 equiv), **4** (1.5 equiv), CH_2Cl_2, rt, overnight, 80% (over 3 steps).

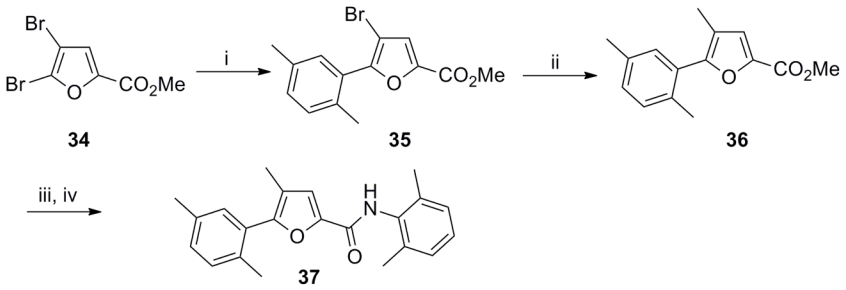

Scheme 8. Synthesis of 2,4,5-trisubstituted furan analog 37

Reagents and conditions: (i) $Pd(OAc)_2$ (0.05 equiv), Cy_3P (0.1 equiv), **16** (1.4 equiv), K_3PO_4 (3 equiv), toluene/H_2O (8:1). 100 °C, 12 h. 40%; (ii) $Pd[(Po\text{-}Tol)_3]_2Cl_2$ (0.05 equiv). Me_4Sn (2 equiv), DMA, 90 °C, 6 h, 65%; (iii) LiOH (1.2 equiv), THF/MeOH/H_2O (2: 2:1); (iv) (a) $(COCl)_2$ (1.3 equiv), DMF, CH_2Cl_2, rt, 2 h; (b) Et_3N (2 equiv), **4** (2 equiv), rt, overnight, 78% (over 3 steps).

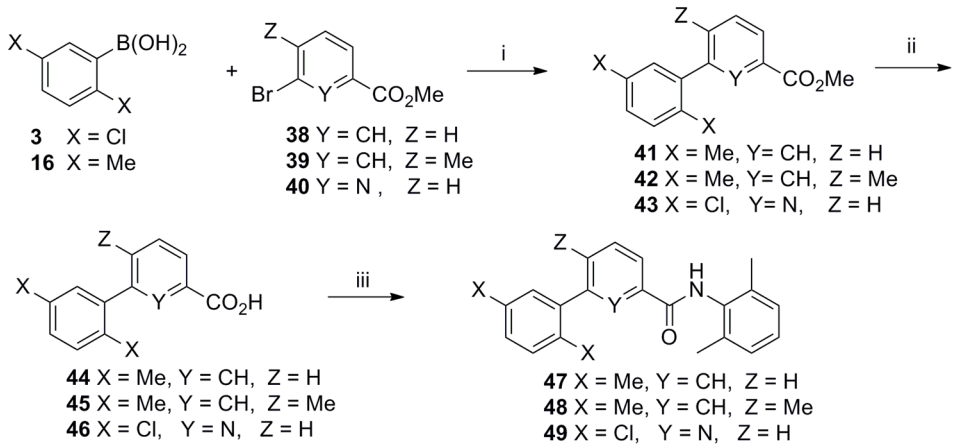

Scheme 9. Synthesis of phenyl and pyridine analogs 47–49

Reagents and conditions: (i) **3** or **16** (1.5 equiv), $Pd(OAc)_2$ (0.05 equiv), Cy_3P (0.1 equiv), K_3PO_4 (3 equiv), toluene/H_2O (8:1), 100 °C, 12 h. 40–75%: (ii) LiOH (1.3 equiv), THF/MeOH/H_2O (2: 2:1). rt, 3 h;(iii) (a) $(COCl)_2$ (1.3 equiv), DMF, CH_2Cl_2, rt, 6 h; (b) Et_3N (2 equiv), **4** (2 equiv), CH_2Cl_2, rt, overnight, 60–85% (over 3 steps).

Table 1

S1P4 antagonist activity of synthesized molecules

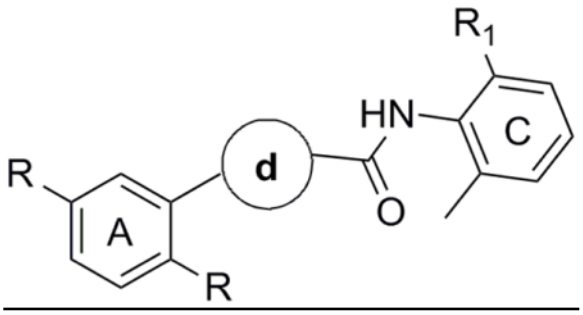

cpd	R	d	R^1	IC_{50} (nM)[α]
1a	Cl	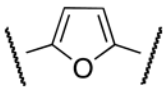	Me	78
1b	Me	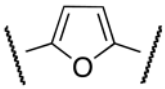	Me	64
9	Cl	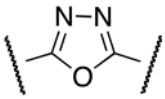	Et	NA
14	Me	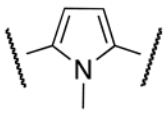	Me	6300
19	Me	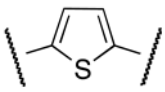	Me	59
23	Me	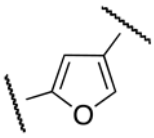	Me	233
28	Me	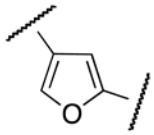	Me	211
33	Me	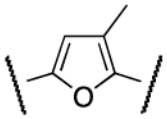	Me	173

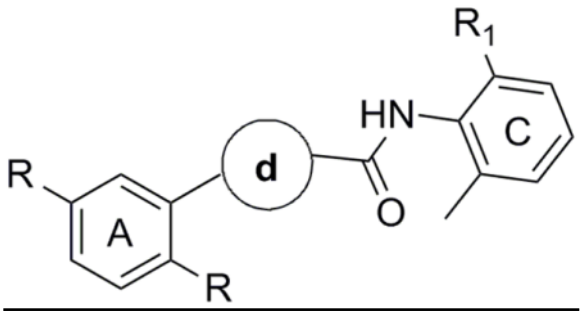

cpd	R	d	R^1	IC_{50} (nM)[α]
37	Me	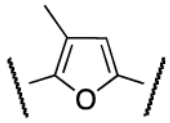	Me	911
47	Me	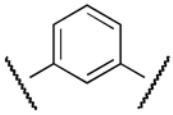	Me	75
48	Me	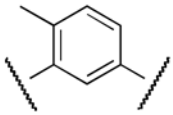	Me	2400
49	Cl	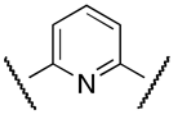	Me	NA

[α]Data are reported as mean for *n* = 3 determinations. NA = not active at concentrations up to 25 μM.

Table 2

S1P selectivity counter screen of compounds **19**, **47**

cpd	IC_{50} (nM)[a]				
	$S1P_4$	**$S1P_1$**	**$S1P_2$**	**$S1P_3$**	**$S1P_5$**
19 (**CYM50333**)	59	NA	1100 (40%)[b]	35%[c]	30%[c]
47 (**CYM50367**)	75	30%[c]	25%[c]	40%[c]	40%[c]

[a] Data are reported as mean for $n = 3$ determinations.

[b] Percentage of inhibition.

[c] Percentage of inhibition at 25μM. NA = not active at concentrations up to 25 μM.

Bioorg Med Chem Lett. Author manuscript; available in PMC 2012 September 15.